SAND2011-7067C

MEMS Resonators with Extremely Low Vibration and Shock Sensitivity

Bongsang Kim, Roy H. Olsson III, Kevin Smart and Kenneth E. Wojciechowski
MEMS Technologies Department, Sandia National Laboratories, Albuquerque NM, USA
bonkim@sandia.gov

Abstract—**MEMS resonator-based oscillators have demonstrated extreme low susceptibility to acceleration. Specifically, oscillators were built employing 100nm-gap electro-statically transduced polysilicon MEMS resonators. An oscillator based upon the Lamé-mode of a square-shaped resonator anchored at four corners demonstrated a measured acceleration sensitivity of $\Gamma_{in-plane}$=2.1ppb/g and $\Gamma_{out-of-plane}$=3.8ppb/g. An oscillator referencing the same design resonator with an additional anchor at the center measured even lower acceleration sensitivity by 5×, $\Gamma_{out-of-plane}$=0.74 ppb/g. These measured values are on-par with the current low-G sensitivity quartz-based oscillators. In separately performed drop tests, these oscillators have shown only -7.7 ppm frequency deviation through an 11,000G impact, which corresponds to an acceleration sensitivity of 0.70 ppb/g. Such extremely low sensitivity to vibrations and shocks enables the use MEMS resonators in environments with extremely high accelerations such as in military and aerospace applications.**

I. INTRODUCTION

To date, MEMS resonators have demonstrated many performance benefits [1]. In particular, capacitive transduction is one of the most popularly used transducer mechanisms for MEMS resonators. Capacitive (or electrostatic) transduction allows avoiding direct contact of the resonator body with electrodes, therefore achieving extremely high quality factors (Q>10,000 or even higher), which is essential for many important emerging applications such as high precision sensors and frequency reference timing devices.

Recently there have been several technical breakthroughs in these types of resonators [1]. For example, strategically designed small anchors have been employed to suspend the resonator structure while minimizing energy loss. Extremely narrow electrode-to-resonator gaps (100nm or even smaller) were developed as another key technology to maximize the transduction efficiency. However, these techniques raise concerns regarding susceptibility to acceleration, which could limit the resonator performance operating in vibrating or high shock environments. Recent studies on capacitively transduced resonators have reported their acceleration sensitivities in the range of 10^{-7}~10^{-8}/g [2, 3]. These values are already comparable to mid-grade commercial quartz-based resonators, but still not as good as SC-cut quartz crystal resonators.

This work is an extended study of our previous works in [3] and [4]. To improve acceleration sensitivity even further, we have improved the anchor designs. Specifically, square-shaped MEMS resonators were suspended by four short support beams attached at their quasi-nodal corners. In some devices, another anchor was added at the center of the resonator body. In the manuscript, various potential mechanisms that may affect acceleration sensitivity of capacitively transduced micromechanical resonators will be briefly revisited. Then measured acceleration sensitivities of oscillators referencing those resonators will be presented. In addition, the result of an extremely high shock test at 11,000g will be also presented.

This work was supported by the Laboratory Directed Research and Development (LDRD) program at Sandia National Laboratories. Sandia National Laboratories is a multiprogram laboratory operated by the Sandia Corporation, Lockheed Martin Company, for the United States Department of Energy's National Nuclear Security Administration under contract DE-AC04-94AL850000.

II. MECHANISMS

In a mechanical resonating structure, external acceleration can affect the natural vibration frequency of the structure. In such a case, the measure of frequency shift, *Δf,* due to acceleration, $\bar{a}$, the acceleration sensitivity, $\bar{\Gamma}$, is often used,

$$\frac{\Delta f}{f} = \bar{\Gamma} \bullet \bar{a} \quad with \quad \bar{\Gamma} = \Gamma_x \hat{x} + \Gamma_y \hat{y} + \Gamma_z \hat{z} \qquad (1)$$

where, f is the natural resonance frequency at rest. Note that both $\bar{\Gamma}$ and $\bar{a}$ are in vector form and orientation dependent.

There are several potential mechanisms that can yield acceleration-induced frequency shifts in capacitively transduced resonators. In this work, some of the important mechanisms are briefly discussed. More details can be found in [3].

A. Acceleation-Induced Stress Effect

Usually, capacitively transduced MEMS resonators are suspended from the substrate by small anchors. As the resonator experiences external acceleration, the inertial force acts on the suspended resonator body, which generates stress near the anchoring points. This induced stress yields a shift in resonant frequency. In general, larger devices are more vulnerable to this mechanism because of the amount of inertial force, and therefore the induced stress amplitude is proportional to the resonator mass. Also the location of the anchor plays a crucial role. If stress is induced in areas where there is large strain at resonance, it impedes its natural resonance more, resulting in larger shifts in resonant frequency.

B. Acceleation-Induced Change in Spring Softening

Spring softening is a well known nonlinear dynamic phenomenon in capacitive transducers. Fig. 1 illustrates this effect

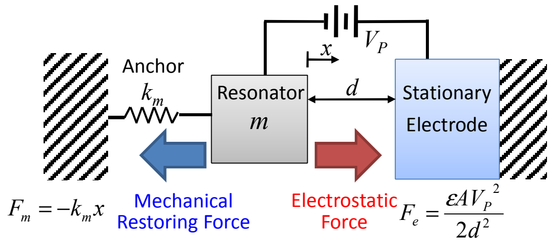

Figure 1. Conceptual schematic of spring softening effect in capacitively transduced MEMS resonators.

between a moving resonator and a stationary electrode spaced with a gap size, *d*. The electrostatic force generated by a constant bias voltage, V_P, applied across the gap increases as the resonator approaches the electrode, i.e., as the gap decreases. And this force decreases as the resonator moves in the opposite direction, i.e., farther from the electrode (gap increases). Since the change in force is proportional to displacement, it can be modeled as an effective electrical stiffness, k_e, as,

$$k_e = \frac{\partial F_e}{\partial x} = \frac{\varepsilon A V_P^2}{d^3} \quad (2)$$

where ε and *A* are the permittivity and overlap area, respectively, of the resonator-to-electrode gap. Since it acts against the restoring force of the resonator's mechanical stiffness, k_m, k_e subtracts from the overall stiffness of the resonator structure, *k*, yielding a resonance frequency given by

$$f = \frac{1}{2\pi}\sqrt{\frac{k}{m}} = \frac{1}{2\pi}\sqrt{\frac{k_m - k_e}{m}} = f_n\sqrt{1 - \frac{k_e}{k_m}} \quad (3)$$

where, *m* is the resonator mass, and f_n is the natural frequency.

If there is any change in the electrical stiffness, Δk_e, due to external acceleration or change in bias voltage, it results in a shift in resonant frequency which can be expressed as,

$$\frac{\Delta f}{f} \approx -\frac{1}{2}\frac{\Delta k_e}{k_m} \quad (4)$$

C. *Electronics and Interconnect Acceleration Sensitivity*

Usually, applications of MEMS-based resonators, such as sensors and signal processors, contain several microwave electronic components at the system level, and many of these are known to be sensitive to acceleration as well. For example, coaxial cables typically exhibit 10^{-4}~10^{-6}rad/g [5]. Also other circuit components such as band-pass filters, mechanical phase shifters, and printed circuit boards change their performance characteristics in the presence of acceleration [6]. Often, such non-resonant circuit components turn out to be dominating the acceleration sensitivity of the entire system.

III. Design and Analysis

A. *Resonator Design and Fabrication*

To investigate the acceleration sensitivity of capacitively transduced MEMS resonators, Lamé-mode square resonators were designed in this work. The length of the square is 67.5µm targeting a resonant frequency of 52 MHz. The resonator structure is suspended from the substrate by four 4.5µmL × 2µmW beam supports at the corners, which are quasi-nodal points at the Lamé resonance mode. For some devices, another cylindrical anchor with a diameter of 4µm was added at the center underneath the device. The resonator mode shape is shown in Fig 2a. The devices were fabricated in a 2.15µm-thick polycrystalline silicon film as shown in an SEM image in Fig. 2b. The electrode-to-resonator gap was defined as 100 nm uniformly by the oxide sacrificial spacer.

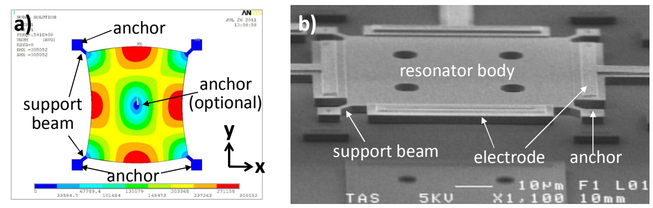

Figure 2. a) ANSYS FE simulated Lame mode shape of the square resonator (top-view). b) An SEM image of the fabricated resonator.

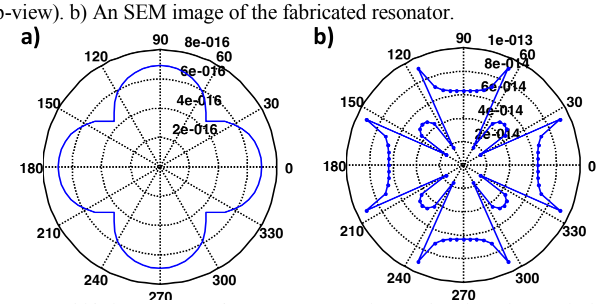

Figure 3. Shift in resonant frequency per unit acceleration due to induced stress effect modeled by ANSYS FE simulation of (a) four anchored devices and (b) five anchored devices depending on the orientation of excitation.

B. *Predicted Acceleration Sensitivity*

The acceleration sensitivity of the micromechanical resonators was estimated using the models described in Section II.

First, the effect of acceleration-induced stress was evaluated using ANSYS FE modeling. From simulation, the in-plane acceleration sensitivity of the four anchored resonator was estimated in the range of $\Gamma_{in\text{-}plane} = 10^{-15}$~$10^{-16}$/g and out-of-plane acceleration sensitivity was estimated as $\Gamma_{out\text{-}of\text{-}plane} = 2.42\text{x}10^{-12}$. In the case of five anchored devices, the in-plane acceleration sensitivities were predicted to be higher, $\Gamma_{in\text{-}plane} = 10^{-13}$~$10^{-14}$/g, but the out-of-plane acceleration sensitivity is lower, $\Gamma_{in\text{-}plane} = 10^{-13}$~$10^{-14}$/g. See Fig. 3 for more detail.

Also the effects of changes in spring softening under acceleration were evaluated. As shown in Fig 4a, the shift in resonant frequency was measured while sweeping the bias voltage, V_P, and from this measured data, by using (2) and (4), the ratio between these two stiffness values were extracted as,

$$k_e / k_m = 5.6 V_p^{\,2} \quad (5)$$

Fig.4b and c illustrates the conceptual schematics that describe resonator displacement in the presence of acceleration.

For in-plane accelerations, the resonator moves to change the resonator-to-electrode gap size. However, as shown in Fig. 4b, while gap size on one side is being reduced, the gap size of the other side increases at the same rate. As a result, k_e increases on one side, but decreases on the other side, therefore, the overall resonator stiffness contribution from electrical stiffness can be expressed as the difference between these two:

$$\Delta k_e = \Delta k_{e,+} - \Delta k_{e,-} = \frac{3}{2}k_e\left(\frac{\delta_x^{\,2} + \delta_y^{\,2}}{d^2}\right) \quad (6)$$

where, δ_x and δ_x are the dislocation magnitude of the resonator structure along x and y direction due to acceleration.

Combining equation (4), (5), and (6) yields,

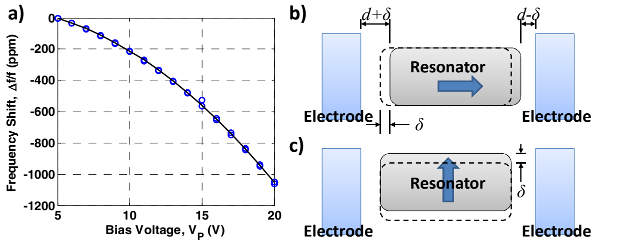

Figure 4. a) Measured frequency shift vs. bias voltage. Conceptual schematics of resonator displacement in the presence of acceleration along (b) the in-plane direction and (c) the out-of-plane direction. Both b and c are side views.

$$\frac{\Delta f}{f} = -4.2 \cdot V_p^{\ 2} \left(\frac{\delta_x^{\ 2} + \delta_y^{\ 2}}{d^2} \right) \tag{7}$$

Since the dislocation magnitudes are proportional to the amplitude of the acceleration, from (7) it can be observed that the shift in resonant frequency is proportional to the square of the acceleration amplitude, therefore, from its definition in (1), the acceleration sensitivity due to change in the spring softening scales up as the amplitude of the acceleration increases.

Using ANSYS FEM, the maximum in-plane resonator dislocations were estimated 1.3×10^{-6} nm (four anchored device) and 4.2×10^{-7} nm (five anchored device) per unit acceleration when excited along either the x- or y-direction. Combining these simulation results with (7), for a 10g-acceleration and V_p = 5~20V, the in-plane acceleration sensitivities due to spring softening are estimated as $\Gamma_{in\text{-}plane}$ = 10^{-14}~10^{-15}/g (four anchored device) and $\Gamma_{in\text{-}plane}$ = 10^{-18}~10^{-19}/g (five anchored device), respectively. Five anchored devices were predicted to exhibit much lower acceleration sensitivity, because the additional anchor at the center provides much higher rigidity.

It is likely that the out-of-plane acceleration sensitivity due to change in spring softening is minimal, since the resonators used in this study were fabricated such that there is little change in either gap spacing or transduction overlap area in the presence of out-of-plane acceleration (see Fig. 4c).

Based on the above analysis, the in-plane acceleration sensitivity of the four anchored device is likely dominated by the change in spring softening, whereas the induced stress dominates in-plane acceleration sensitivity of the five anchored device. For out-of-plane accelerations, both devices are likely dominated by the induced stress. Note that all of the values predicted above are several orders of magnitude smaller than even state-of-the-art SC-cut quartz crystal-based resonators. Such low acceleration sensitivities are contributed by both the very tiny mass of micromechanical resonators, ~23pg, minimizing the amount stress gradient and resonator dislocation induced by external acceleration, and also strategic placements of anchors at resonator quasi-nodal points, which minimizes the effect of generated stress on the resonant frequency.

IV. Acceleration Sensitivity Measurement

One of the most effective ways to measure resonator acceleration sensitivity is to build an oscillator loop referencing the resonator and investigate the output power spectrum while the resonator is excited by periodic vibrations.

When a resonator-based oscillator experiences a vibration at a fixed frequency, f_v, the output signal phase is modulated by the instantaneous resonant frequency shift of the resonator, creating sideband peaks in the output power spectrum. Since only the carrier power constitutes the oscillator output, and everything else is noise, the side peaks can be interpreted as phase noise at a frequency offset of f_v from the carrier, and their relative heights, L, can be expressed as,

$$L(f_V) = 20\log\left(\frac{(\overline{\Gamma} \bullet \overline{a}) \cdot f}{2 f_v} \right) \tag{8}$$

Therefore, by measuring the amplitude of the side band peaks, acceleration sensitivity, Γ, can be calculated using (8).

Fig. 5a illustrates the experimental setup used for acceleration sensitivity measurement of oscillators referenced to the polysilicon MEMS resonators. A Bruel & Kjaer Type 4809 shaker, to which the PCB was attached, provides periodic vibrations, while the oscillator output power spectrum was measured. The oscillator loop consists of a MEMS resonator together with two Philips NE5211 transimpedance amplifiers in series to obtain 360° phase shift and the required gain around the loop. The fabricated printed circuit board (PCB) is shown in Fig. 5b. In the PCB, two MEMS-based accelerometers (Analog Device AD22286 and Freescale MMA1213D) were also mounted close to the resonator to monitor the level and the orientation of the applied acceleration.

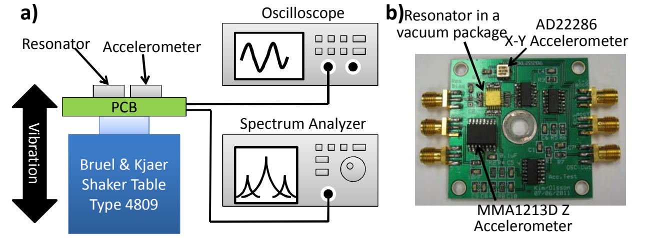

Figure 5. a) Schematic of acceleration sensitivity test setup. b) A picture of oscillator PCB. A MEMS resonator is enclosed in a vacuum package.

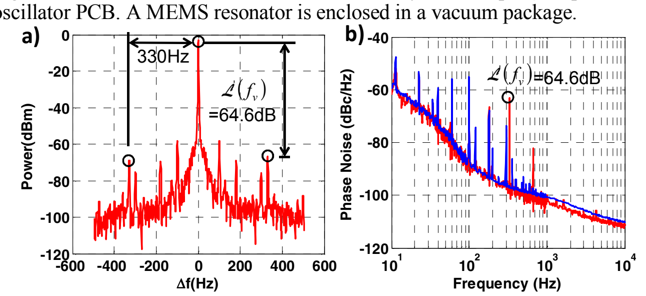

Figure 6. (a) Output power spectrum and (b) phase noise measurement plots of an oscillator with a four anchored device with excitation (red) and at rest (blue). The peaks heights from both measurements match each other. V_P = 5V, $Acc.X$ = 2.38g, $Acc.Y$ = 1.85g, $Acc.Z$ = 3.31g, and f_v = 330Hz

The oscillator began oscillating at a bias voltage as low as 5V, and the side band peak heights at the output were measured by both an HP4396B spectrum analyzer and a Symmetricom 5125A phase noise analyzer. Fig 6a and Fig 6b present example measured plots from the spectrum analyzer and the phase noise analyzer, respectively.

Table 1 summarizes the measured side peak heights of the oscillator using a four anchored resonator while it is excited in five different orientations. Using this data, together with (8) and the root mean square method, each vector component of acceleration sensitivity, $\overline{\Gamma}$, can be extracted. For better understanding, the in-plane acceleration sensitivities were decom-

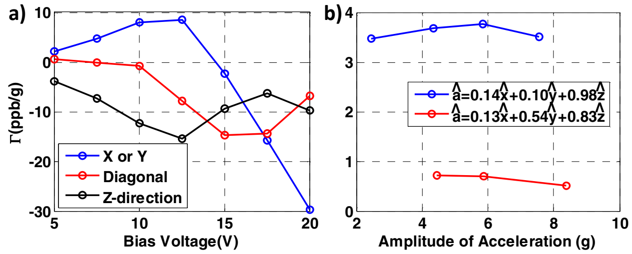

Figure 7. a) Extracted acceleration sensitivity along three major acceleration orientation X or Y, diagonal, and Z (out-of-plane) with respect to bias voltage. (Measured at f_v = 330Hz) b) Acceleration amplitude dependence of acceleration sensitivity measured for two different excitation orientations. In both along $0.14\hat{x}+0.10\hat{y}+0.98\hat{z}$ direction and $0.13\hat{x}+0.54\hat{y}+0.83\hat{z}$ direction, no clear trend could be found. (Measured at V_P = 5V and f_v = 330Hz)

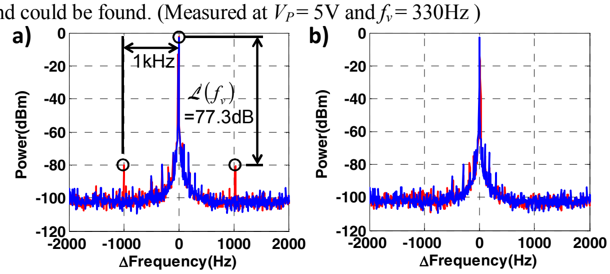

Figure 8. Output power spectrum of five anchored device when excited (red) along a) out-of-plane at 10g and b) in-plane at 20g and at rest (blue). For the in-plane measurement, any side-band peaks above noise level could be found even at 20g acceleration. V_P = 4V and f_v = 1000Hz for both tests.

posed into x- or y-directions and the diagonal direction. For example, at V_P = 5V, the oscillator with a four anchored device exhibited acceleration sensitivities of $\Gamma_{x\ or\ y}$ = 2.2 ppb/g, $\Gamma_{diagonal}$ = 0.64 ppb/g, and $\Gamma_{out\text{-}of\text{-}plane}$ = 3.8 ppb/g. The extracted acceleration sensitivity components for each orientation with respect to bias voltage are summarized in Fig 7a.

An oscillator with a five anchored device was also tested. Its out-of-plane acceleration sensitivity was measured $\Gamma_{out\text{-}of\text{-}plane}$ = 0.74 ppb/g (see Fig. 8), about 5× smaller than the oscillator with a four anchored resonator. The in-plane acceleration sensitivity could not be measured at the time of writing due to the noise-level of the spectrum analyzer. Considering -90 dB noise-floor of the current test setup, the in-plane acceleration sensitivity of the oscillator with a five anchored device is presumably 0.17 ppb/g or less. Currently we are working to improve the measurement setup.

V. Shock Test

A shock-test was conducted using a drop test setup as shown in Fig 9a. The oscillator was still performing as before even after experiencing eight shocks (drops) of 5,000g and another four shocks of 11,000g. Fig. 9b shows the measured output frequency during the shock test. The maximum frequency deviation was observed as -7.7 ppm, 1.7 msec after the impact, which corresponds to a 0.70 ppb/g acceleration sensitivity. This 1.7 msec of delay infers that the oscillator acceleration sensitivity could possibly be dominated by its cabling or wire-bonds instead of the MEMS resonator.

TABLE I. Summary of measured side band peak heights of the oscillator output power with a four anchored device. The PCB was excited at 330Hz while varing bias voltage from 5V to 20V.

Acceleration (G, RMS)			Measured Side Band Peak Heights, *L* (dB)						
			Bias Voltage						
ACC.X	*ACC.Y*	*ACC.Z*	*5V*	*7.5V*	*10V*	*12.5V*	*15V*	*17.5V*	*20V*
3.34	0.35	2.79	-70.0	-65.1	-59.8	-54.1	-49.6	-44.8	-40.3
2.38	1.85	3.31	-62.4	-59.1	-56.4	-54.9	-55.4	-56.5	-55.8
3.66	3.41	4.90	-58.2	-50.8	-45.6	-41.2	-42.6	-45.5	-48.9
0.47	0.27	3.29	-60.2	-55.2	-49.7	-46.9	-47.7	-48.9	-49.0
0.52	0.32	2.39	-63.4	-57.8	-53.9	-51.9	-56.4	-59.0	-58.6

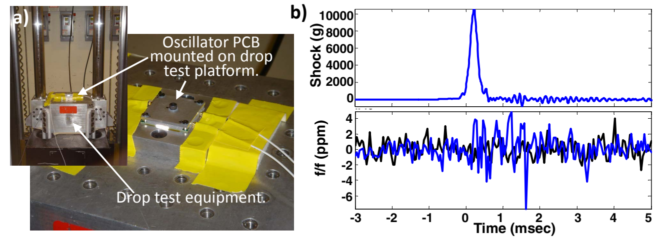

Figure 9. a) A picture of shock test setup. b) Applied acceleration time profile and the measured oscillator frequency deviation during shock (blue) vs. at rest (black). The maximum $\Delta f/f$ of -7.7ppm was observed 1.7msec after the impact.

VI. Conclusion

Acceleration sensitivities of MEMS-based oscillators were measured in the ppb/g (four anchored device) to even sub-ppb/g ranges (five anchored device). These measured values are comparable with SC-cut quartz-based oscillators and much better than the values reported in the previous works on MEMS-based oscillators [2, 3], however still several orders of magnitude higher than those predicted by the models.

The oscillator using a four anchored device measured the least sensitive to acceleration along its diagonal direction as can be seen in Fig. 7a. At low bias voltage, out-of-plane acceleration sensitivity is the largest, but as the bias voltage increases, soon the x- or y- direction sensitivity dominates the overall oscillator acceleration sensitivity. These results postulate spring softening could be the dominant mechanism for the acceleration sensitivity of capacitively transduced MEMS resonator-based oscillators, however, in a preliminary test shown in Fig. 7b, no clear trend on the acceleration sensitivity with respected to the acceleration amplitude could be found, which is contradictory to the observation of (7).

It is not yet clear whether the MEMS resonator itself dominates the acceleration sensitivity of the measured oscillators. As discussed in Section II, often non-resonating circuit components dominate the system-level acceleration sensitivity [6], therefore still it is possible that the discrepancy between the models in Section II and the measured data in Section III is not due to the MEMS resonator, in which case, integration of MEMS resonators with circuitry [7] would be able to significantly improve the acceleration sensitivity limits of MEMS resonator-based systems.

Currently, further investigation is being pursued to shed light on the exact mechanisms of acceleration sensitivity of MEMS resonator based oscillators.

References

[1] C. T.-C. Nguyen, *IEEE Trans.on UFFC,* vol. 54, pp. 251-270, 2007

[2] M. Agarwal, *Applied Physics Letters,* vol. 90, p. 3, Jan 2007

[3] B. Kim, *IEEE FCS*, Newport Beach, USA 2010, pp. 273-278

[4] K. Wojciechowski, *IEEE FCS*, Geneva, Switzerland, 2007, pp.1220-4

[5] A. Hati, *IEEE FCS*, Geneva, Switzerland, 2007, pp. 541-546

[6] M.M. Driscoll, *IEEE FCS*, Geneva, Switzerland, 2007, pp. 535-540

[7] Huang, IEEE MEMS Conference, 2008, pp. 10-13